Supporting Information

Long-Term Stable Zero-Thermal-Quenching Blue-Emitting Phosphor for Sustainable and Human-Centric Lighting

Heng Dai [a,b], Xinran Wang [a], Zhichao Liu [a], Jian Zhang [a], Xuhui Xu [a*], Ge Zhu [b*]

[a] Yunnan Joint International Laboratory of Optoelectronic Materials and Devices, Faculty of Materials Science and Engineering, Kunming University of Science and Technology, Kunming Yunnan 650093, Yunnan, China
[b] Key Laboratory of New Energy and Rare Earth Resource Utilization of State Ethnic Affairs Commission, Key Laboratory of Photosensitive Materials & Devices of Liaoning Province, College of Physics and Materials Engineering Dalian Minzu University 18 Liaohe West Road, Dalian 116600, P. R. China

Corresponding Authors

E-mail addresses: xuxuh07@126.com (Xuhui Xu); zhuge@dlnu.edu.cn (Ge Zhu)

Experimental section

Synthesis: A series of SMAO: xEu^{2+} ($0 \leq x \leq 0.02$) phosphors were synthesized by the high temperature solid-state method. The stoichiometric raw materials $SrCO_3$ (99.99%), $4MgCO_3 \cdot Mg(OH)_2 \cdot 5H_2O$ (98%), Al_2O_3 (99.99%), and Eu_2O_3 (99.99%) were well mixed in an agate mortar and collect to the alumina crucible. The mixture was sintered at a reduced atmosphere of 1400°C (H_2:N_2 = 5:95) for 6 h and then carefully ground with porcelain for further characterization at room temperature.

Characterization: The as-prepared samples were tested for phase structure on a Shimadzu model DX-2700BH X-ray diffractor using Cu-Kα radiation (λ = 0.15406 nm) under 40 kV and 30 mA. Refinement of the diffraction data was performed by the General Structural Analysis System (GSAS) software. The diffuse reflectance spectra (DRS) of the samples were determination by UV-Vis-NIR spectrophotometer (Shimadzu UV-3600). The morphology of the sample was investigated using field emission scanning electron microscopy (SEM, S-4800). The energy dispersion X-ray spectra (EDS) and elemental maps were determination using the same SEM instrument. Photoluminescence excitation (PLE) and photoluminescent (PL) spectra were recorded at room temperature on an Edinburgh spectrum of FS5-MCS, with a 450 W Xe lamp as a light source. High resolution transmission electron microscopic (HR-TEM) images were characterized on a FEI TECNAI G2 F20 microscope with an accelerate voltage of 200 kV. Variable temperature emission spectra were determination using the FS5-MCS spectrometer, which used temperature

control devices as control accessories. The internal quantum efficiency (IQE) was measured using the integrated sphere on FLS1000 instrument, and the white $BaSO_4$ powder was used as the reference. The Thermoluminescence (TL) curve was quantified by heating with an FJ-427A1 instrument at a frequency of 3 K/s. A Thermos Fisher X-ray photoelectron spectrometer was applied to explore the X-ray photoelectron spectra (XPS) under less than 10^{-7} Pa of ultrahigh vacuum while using Al-Kα X-ray radiation. Electron paramagnetic resonance (EPR) spectrum was recorded by a JES-FA200 ESR Spectrometer USH-500SC.

Table S1. Refined crystallographic parameters of SMAO: $0.015Eu^{2+}$ phosphor.

Formula	**SMAO: $0.015Eu^{2+}$**
Crystal system	Hexagonal
Space group	$P\bar{6}m2$
a/b (Å)	5.583
c (Å)	22.116
V (Å^3)	598.832
R_{wp} (%)	13.86
R_p (%)	9.94
χ^2	1.68

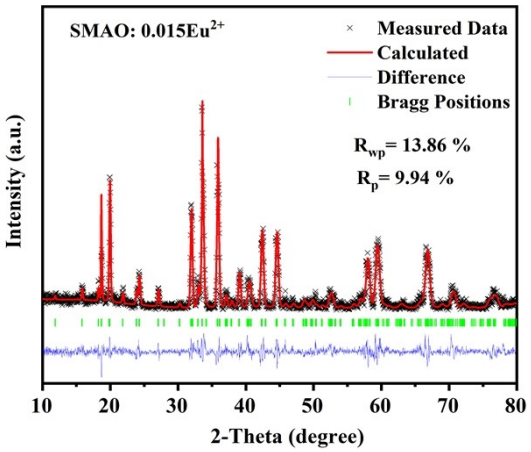

Fig. S1. The refinement detailed graph of SMAO: $0.015Eu^{2+}$.

Table S2. Atomic site occupation of SMAO: $0.015Eu^{2+}$ phosphor obtained by the Rietveld refinement.

Atom	**Wyckoff**	**x**	**y**	**z**	**Occ.**	**U[Å^2]**
Sr1	1e	0.6667	0.3333	0	1	0.6205
Sr2	3k	0.3305	0.6554	0.5	0.303	0.0087
Al1	6n	0.8535	0.6419	0.1411	0.710(0)	0.0105
Al2	6n	0.1667	0.3334	0.3532	0.290(0)	0.0178
Al3	2h	0.3333	0.6667	0.2208	0.667	0.0064
Mg1	2h	0.6667	0.3333	0.2387	0.333	0.0064
Al4	2i	0.6667	0.3333	0.2735	1.000(0)	0.0435
Al5	2h	0.3333	0.6667	0.0645	1.000(0)	0.0405
Al6	2i	0.6667	0.3333	0.4324	1.000(0)	0.0216

Al7	2g	0	0	0.2543	1.000(0)	0.0189
Al8	2g	0	0	0.0194	0.5	0.0262
O1	6n	0.1350	0.3197	0.1978	1.000(0)	0.0150
O2	6n	0.8889	0.7479	0.3018	1.000(0)	0.0512
O3	6n	0.5245	0.0325	0.0937	1.000(0)	0.0180
O4	6n	0.5018	0.9797	0.3911	1.000(0)	0.0443
O5	2i	0.6667	0.3333	0.1853	1.000(0)	0.0035
O6	2h	0.3333	0.6667	0.3210	1.000(0)	0.0120
O7	2g	0	0	0.0939	1.000(0)	0.0083
O8	2g	0	0	0.4153	0	0.6634
O9	3j	0.2424	0.3621	0	0	0.2210
O10	3k	0.5686	0.2845	0.5	0.333	0.6715

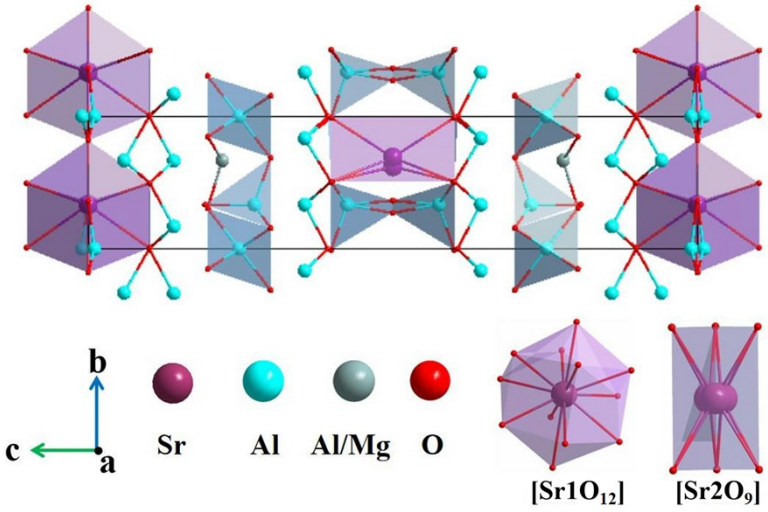

Fig. S2. The crystal structure and polyhedral combination diagram in SMAO host.

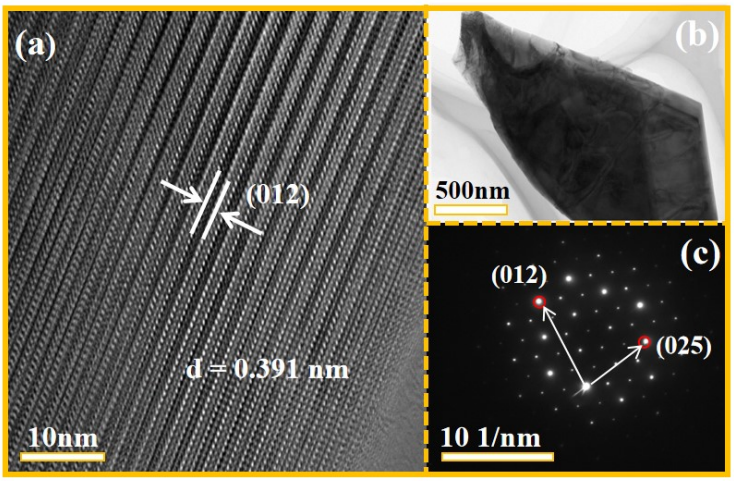

Fig. S3. (a) HR-TEM pattern; (b) TEM image of the phosphor particle; (c) Corresponding FFT image.

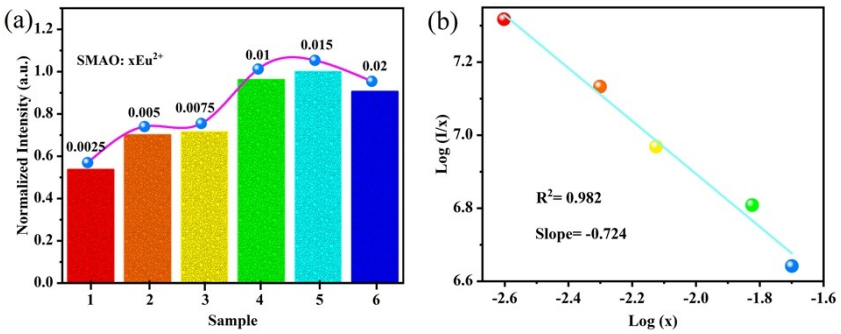

Fig. S4. (a) Emission intensity of the SMAO: xEu^{2+} ($0.0025 \leq x \leq 0.02$) phosphors as a function of content; (b) Plot of Log (I/x) vs. Log (x) for the SMAO: xEu^{2+} ($0.0025 \leq x \leq 0.02$) phosphors.

According to the best doping concentration, the critical distance (R_c) can be obtained using the following equation,[1]

$$R_c = 2 \times \left(\frac{3V}{4\pi x_c Z} \right)^{\frac{1}{3}} \qquad (1)$$

where x_c is a critical concentration, Z is the number of activator ions occupation number in the unit cell, and V represents the volume of the unit cell. In SMAO: Eu^{2+}, Z is 1 and V is 598.83 Å^3. R_c is determined to be 42.41 Å. When $R_c < 5$ Å, the exchange interaction is dominant, in contrast, when $R_c > 5$ Å, the multidipole interaction is responsible for the energy transfer.[1] Thus, the luminescence is mainly due to electric multidipole interactions between Eu^{2+} ions in SMAO crystals. The interaction types between Eu^{2+} can be obtained by equation,[2]

$$\frac{I}{x} = K \left[1 + \beta (x)^{\frac{\theta}{3}} \right]^{-1} \qquad (2)$$

where I is the emission intensity and x is the activator concentration, k and β were constants associated with the matrix and interaction type. The value of θ represents different types of electric multipolar interaction. $\theta = 6$, 8, and 10 corresponds to dipole-dipole (d-d), dipole-quadrupole (d-q), quadrapole-quadrapole (q-q) interactions, respectively. Fig. S2b gives the linear relationship between log (I/x) and log (x), and the slope by linear fitting (-θ/3) was -0.724. Accordingly, the value of θ is 3.172, which is close to 6, indicating that the dipole-dipole interaction plays a dominant role in the energy transfer process in the SMAO: xEu^{2+} ($0.0025 \leq x \leq 0.02$) system.

The decay curves of SMAO: xEu^{2+} ($0.0025 \leq x \leq 0.02$) phosphors can be fitted by the following double exponential equation well,[3]

$$I(t) = A_1\exp(-\frac{t}{\tau_1})+A_2\exp(-\frac{t}{\tau_2}) \qquad (3)$$

where $I(t)$ is emission intensities at times t, A_1, A_2 are constants, and τ_1, τ_2 represent the lifetimes. The lifetime τ decreases significantly when the Eu^{2+} concentration increases from 0.0025 to 0.02.

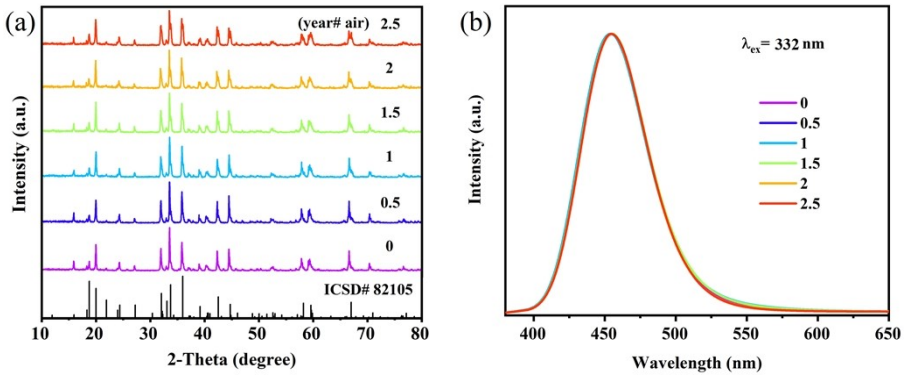

Fig. S5. The (a) powder X-ray diffractograms and (b) Normalized emission spectra of SMAO: 0.015Eu^{2+} upon 332 nm excitation after 0, 0.5, 1, 1.5, 2 and 2.5 years of place in air.

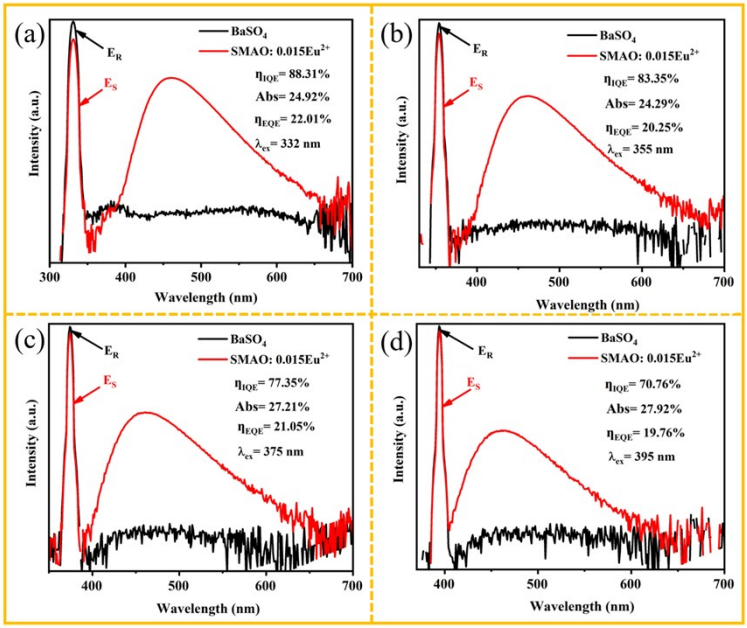

Fig. S6. (a-d) The IQE and EQE spectra of the SMAO: 0.015Eu^{2+} phosphor at different excitation wavelengths.

The relationship between the luminous energy of Eu^{2+} ion and the coordination environment is expressed by the following equation,[4]

$$E = Q\left[1-(\frac{V}{4})^{\frac{1}{V}}10^{\frac{-nE_a r}{80}}\right] \qquad (4)$$

where Q and V are constants for Eu^{2+}, and n and r refer to the coordination number and radius of the replaced cation, respectively, while E_a represents the anion's electron affinity. In this case, if values of n and r are larger, their emission energy is larger.

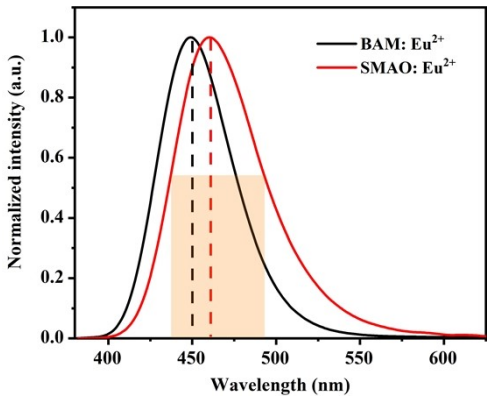

Fig. S7. The emission spectra of SMAO: Eu^{2+} and commercial BAM: Eu^{2+} phosphor.

Typically, the FWHM is related to the electron-phonon coupling effect, which can be evaluated by Huang-Rhys factor (S) by virtue of the formula:[5]

$$\mathrm{FWHM}(T) = 2.36\sqrt{S}\hbar\omega_{phonon}\sqrt{\coth\frac{\hbar\omega_{phonon}}{2k_B T}} \qquad (5)$$

where $\hbar\omega$ is the vibrational phonon energy, S is the Huang-Rhys parameter, k_B is the Boltzmann constant.

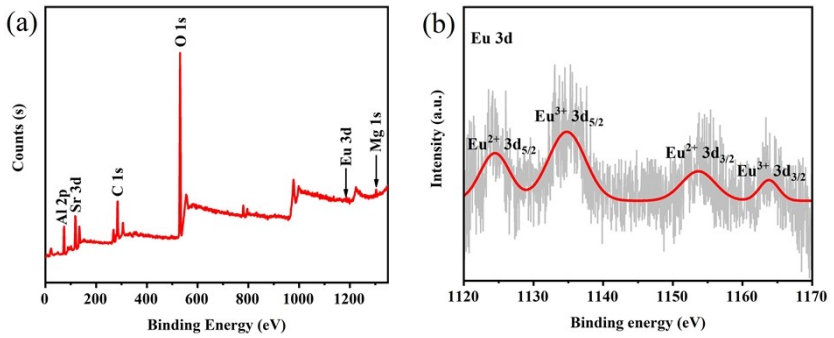

Fig. S8. (a) The XPS survey spectrum of SMAO: $0.015Eu^{2+}$; (b) The XPS spectrum of Eu 3d orbitals.

Table S3. The XPS elemental analysis of SMAO: $0.015Eu^{2+}$.

Element	Sr	Mg	Al	**O**	Eu
Theory (%)	3.13	1.10	36.66	**59.07**	0.04
XPS value (%)	2.96	1.04	35.63	**60.31**	0.06

References

[1] X. Zhang, J. Zhang, X. Wu, L. Yu, Y. Liu, X. Xu and S. Lian, Discovery of blue-emitting Eu^{2+}-activated sodium aluminate phosphor with high thermal stability via phase segregation, *Chem. Eng. J.,* 2020, **388**, 124289.

[2] Z. Li, G. Zhu, S. Li, S. Xin, W. Xu, X. Luo, M. He and B. Dong, Ultra-small stokes shift induced thermal robust efficient blue-emitting alkaline phosphate phosphors for LWUV WLEDs, *Ceram. Int.,* 2023, **49**, 21510.

[3] Q. Xu, J. Meng, K. Sinha, F. Chowdhury, J. Hu and X.Wang, Ultrafast colloidal quantum dot infrared photodiode, *ACS Photonics,* 2020, **7**, 1297.

[4] L. Van Uitert, An empirical relation fitting the position in energy of the lower d-band edge for Eu^{2+} OR Ce^{3+} in various compounds, *J. Lumin.,* 1984, **29**, 1.

[5] H. Jiang, L. Chen, X. Wu, Z. Luo, R. Li, Y. Liu, Z. Liu, P. Sun, W. You and J. Jiang, Spectral regulation and efficiency optimization in Cr^{3+}-doped gadolinium aluminum gallium garnet near-infrared ceramic phosphors via crystal-field engineering, *Adv. Mater. Technol.,* 2022, **7**, 2200519.